Soft Matter

Accepted Manuscript

ROYAL SOCIETY OF CHEMISTRY

www.rsc.org/softmatter

Journal Name

ARTICLE TYPE

Cite this: DOI: 10.1039/xxxxxxxxxx

Directed self assembly of block copolymers using chemical patterns with sidewall guiding lines, back-filled with random copolymer brushes

Gunja Pandav,[a] William J. Durand,[a] Christopher J. Ellison,[a] C. Grant Willson,[ab] and Venkat Ganesan*[a]

Received Date
Accepted Date

DOI: 10.1039/xxxxxxxxxx

www.rsc.org/journalname

Recently, alignment of block copolymer domains has been achieved using a topographically patterned substrate with a sidewall preferential to one of the blocks. This strategy has been suggested as an option to overcome the patterning resolution challenges facing chemoepitaxy strategies, which utilize chemical stripes with a width of about half the period of block copolymer to orient the equilibrium morphologies. In this work, single chain in mean field simulation methodology was used to study the self assembly of symmetric block copolymers on topographically patterned substrates with sidewall interactions. Random copolymer brushes grafted to the background region (space between patterns) were modeled explicitly. The effects of changes in pattern width, film thicknesses and strength of sidewall interaction on the resulting morphologies were examined and the conditions which led to perpendicular morphologies required for lithographic applications were identified. A number of density multiplication schemes were studied in order to gauge the efficiency with which the sidewall pattern can guide the self assembly of block copolymers. The results indicate that such a patterning technique can potentially utilize pattern widths of the order of one-two times the period of block copolymer and still be able to guide ordering of the block copolymer domains up to 8X density multiplication.

1 Introduction

Recently, directed self-assembly (DSA) of block copolymers (BCPs) [1–4] has emerged as a powerful tool to facilitate production of sub 20 nm scale patterns for lithography applications. [5–7] Chemoepitaxy is an approach popularly used to achieve long range order of BCP domains. [8–10] In such a strategy, chemical patterns having a width close to half the domain spacing of the block copolymer, and preferential to one of the blocks of the BCP are used as guiding lines to align the BCP morphologies. [10–14] The background, i.e. the area between the chemical stripes, is backfilled with a grafted brush of random copolymers and is tuned to provide a surface which is approximately equally preferential to both the blocks (neutral). [15,16] The size and spacing of the chemical patterns, the composition of grafted copolymer, and the chemical affinity, i.e., the strength with which the chemical stripe wets the BCP components plays an important role on the resulting morphologies and the degree of alignment that can be achieved. [13] Recent studies have demonstrated that, such chemoepitaxy approaches can multiply the pattern resolution (i.e. achieve defect free alignment of lamellar domains) by a factor known as density multiplication, $M = L_s/L_o$, where L_s is the spacing between the chemical patterns on the substrate and L_o is the period of lamellae forming BCP. [17] The factor M is usually denoted as MX to indicate the extent of multiplication of the aligned lamellar domains achieved by chemoepitaxy processes. For symmetric poly(styrene-b-methyl methacrylate), PS-b-PMMA, DSA has demonstrated near prefect perpendicular morphologies using patterns with $0.5L_o$ width and density multiplication up to 4X. [13] However, such DSA was achieved by tuning the brush composition specifically for each density multiplication scheme. Moreover, if patterns wider than $0.5L_o$ are employed, the width needs to be targeted to $1.5L_o$ and pattern chemistries need an even finer tuning. For instance, too weak or too strong preference for the guiding material was seen to result in lower selectivity for desired morphologies. [14]

Recent advances in high resolution patterning technology by the semiconductor industry and disk drive manufacturers have driven the minimum feature size that must be defined by DSA to very low values. [18] For instance, bit patterned media for hard disk drives [19] and semiconductor device manufacturing require patterning feature sizes below 10 nm. This in turn has spurred interest in block copolymers possessing a large degree of incom-

[a] The University of Texas at Austin, McKetta Department of Chemical Engineering, Austin, TX 78712. E-mail: venkat@che.utexas.edu
[b] The University of Texas at Austin, Department of Chemistry, Austin, TX 78712.

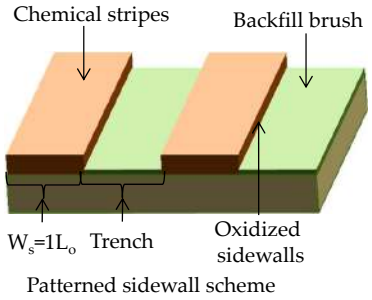

Fig. 1 Schematic of double patterned sidewall guiding scheme.

patibility quantified by a high Flory-Huggins interaction parameter, χ,[20–25] so that low molecular weights can be employed. The transition to such BCPs also brings on a major challenge for chemoepitaxy strategies. Specifically, such advances now necessitate patterning guiding lines which are also on the sub-10 nm scale, which is well beyond the resolution of 193 nm photolithography. Not surprisingly, there has arisen a significant interest in strategies that can employ wider chemical patterns without a concomitant loss in the density multiplication that can be achieved. In addition, chemoepitaxy strategies suffer from the fact that the composition of the backfill brush has to be optimized for each different density multiplication. Approaches that can achieve density multiplication without the need to tune brush compositions are of significant interest.

Recently, a new strategy has been proposed that utilizes a sidewall guiding scheme to relax the pattern resolution requirement for chemoepitaxy.[26,27] This approach combines graphoepitaxy (which employs a shallow trench between polymer mat and backfill brush) with chemoepitaxy (cf. Figure 1). This technique depends on the fact that the oxidized sidewalls of trenches in a neutral polymer are preferential to one of the blocks. Because two guiding surfaces are generated per pattern, a pattern width of the order of L_o (or higher) can be utilized. Cushen *et al.*[27] demonstrated this strategy by using chemical patterns on polystyrene mat having a width of $1L_o$, and were able to guide self assembly up to 3X density multiplication. While the study by Cushen *et al.*[27] was successful in establishing a proof of concept, a number of unresolved questions remain about the applicability of the strategy. For instance, some questions include, "can such an approach reduce requirements for pattern resolution, i.e. can wider patterns be utilized?" If so, "does this scheme enable higher density multiplication?", "can a wide range of density multiplication be achieved for the same brush compositions?" Motivated by such questions, a series of simulations were carried out to explore the effect of sidewall interaction on the DSA of BCPs and identify the conditions that lead to the vertical lamellar morphologies required for nano-patterning applications. For this purpose, the single chain in mean field simulation (SCMF) methodology introduced by Muller and coworkers[28–35] was adopted. SCMF methodology is a Monte Carlo (MC) simulation approach wherein the intramolecular bonded interactions among copolymer segments are treated explicitly whereas the nonbonded interactions such as incompatibility among the blocks and incompressibility are treated indirectly by one-body interactions with potential fields instead of a pairwise computation.[28,29,31–35] Hence, such methods are computationally efficient and enable significant parallelization. The SCMF method has been successfully employed to study phase behavior of polymer blends,[28,36] block copolymers,[29,37–39] polymer nanoparticle mixtures,[40] semiflexible copolymers,[41] and BCP thin films.[31,42–44] In this work, the SCMF method was used to study the effect of pattern width, sidewall preference and backfill brush properties on the self assembly of block copolymers.

The computational aspects of DSA of lamellae-forming BCPs using chemoepitaxy strategies have been well studied.[10,12–14,31,39,42–50] However, a common feature of all these studies has been that the background region has been modeled as a uniform surface with a specified surface energy instead of the more realistic picture of grafted brushes of random copolymers.[10,12–14,31,39,42–48,50] Unlike a hard surface with a specified surface energy, grafted copolymers can modulate their interfacial energies by conformational rearrangements and redistribution of segments. For instance, a previous study using self consistent field theory demonstrated the importance of modeling the random copolymer brush explicitly and the features which arise as a result of this more realistic model.[51,52] In that case, the ends of the grafted chains were seen to exhibit segmental rearrangements to create an energetically favorable interface for the perpendicular morphologies relative to the parallel conformations. In this manner, approximating the effect of brush composition, height and density with a single effective surface energy was demonstrated to be an oversimplification that did not capture the role of the polymer brush on self assembly. Motivated by such considerations, in this work the background region was modeled explicitly as grafted random copolymer brushes in attempt to enable a more realistic characterization of the parameter space for DSA.

2 Simulation Details

2.1 Simulation method and model parameters

Since details of the SCMF framework have been reported in earlier studies, this paper reports only the most essential details of the simulation method. In this model, the system consists of n AB BCP chains each having length $N+1$ confined between two parallel planes having thickness L_z in volume, V. The pattern is modeled as a raised surface having a height, H_s, width, W_s, arranged with a period, L_s. A schematic of the model system is shown in Figure 2. The backfill region consists of n_g AB random copolymer chains of length N_g, with grafting density, σ (the number of random copolymer chains per unit area). The interactions which contribute to the energy of the system involve bonded and nonbonded energy between BCP and random copolymer monomers and the interaction energy of the monomers with hard walls i.e. both the top and sidewalls of the pattern. The BCP chains and random copolymers were modeled as Gaussian chains where the flexible bonds were represented by harmonic springs. The bonded

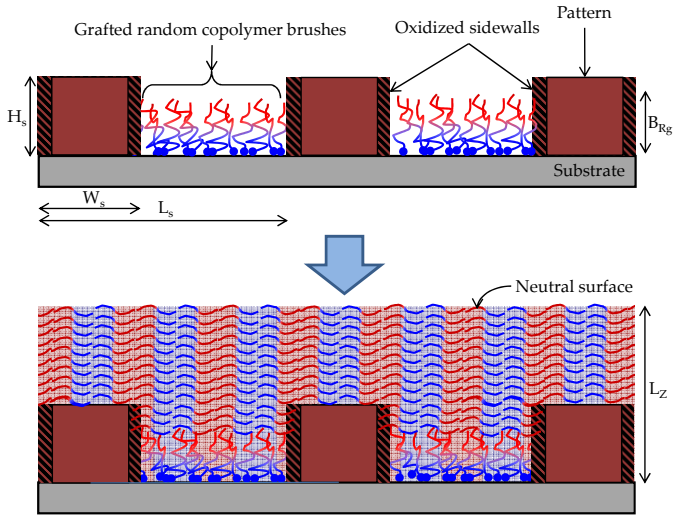

Fig. 2 Schematic of 3X density multiplication scheme with pattern width of 1 L_o with sidewall interactions.

energy, H_b, of this model was given as[53]

$$\frac{H_b[r_i(s)]}{k_BT} = \frac{3}{2b^2}\sum_{i=1}^{n}\sum_{s=1}^{N}\left[[r_i(s)-r_i(s+1)]^2\right] \quad (1)$$

where $r_i(s)$ is the position of s^{th} monomer on the i^{th} chain and b is the bond length between two adjacent monomers given by $b=\sqrt{6R_g^2/N}$ where R_g is the radius of gyration of the polymer chain. The same model with an identical bond length was used for the grafted random copolymer chains. To model the chemistry of the random copolymer chains, an ensemble of compositionally symmetric (on an average) AB random copolymer chains having prespecified sequences was employed. For the sequence distribution of the grafted copolymers, it was assumed that the random copolymers possess an uncorrelated sequence of A and B monomers.[54] In other words, for a symmetric random copolymer chain, each monomer had an equal probability of being an A or a B monomer. In order to closely mimic experimental conditions, the ends of random copolymers were randomly grafted to the surface of the background region.

In SCMF, the nonbonded energy contributions are incorporated as potential fields $w(r_i(s))$ and $\pi(r_i(s))$ that act on the polymer segments. The functional form of these fields is usually taken to correspond to the saddle point solution of the analogous field theory given by,[29,53]

$$w(r) = \frac{\chi N}{2}(\phi_A(r)-\phi_B(r)) \quad (2)$$

$$\pi(r) = \kappa N(\phi_A(r)+\phi_B(r)-1) \quad (3)$$

where ϕ_α $(\alpha = A,B)$ represents the instantaneous local volume fraction of α segments, and κ is a parameter that is inversely proportional to the isothermal compressibility of the overall system.[29] In the above notation, $w_A = -w+\pi$ and $w_B = w+\pi$ are the fields acting on the A and B segments respectively.

The interaction of the monomers with a hard surface was modeled by a short-range potential similar to those used in previous studies[12,17,47,48,50] and was given as

$$\frac{H_s(r_i,K)}{k_BT} = -\frac{\Lambda_i^K(x,y)}{d_s}\exp(\frac{-z^2}{2d_s^2}) \quad (4)$$

where Λ_i^K denotes the strength of interaction of type i (substrate top, sidewall) of the monomer K (A or B) at a position (x,y) with the hard wall and d_s is the range of interaction. For each monomer type, two sets of interaction parameters, viz., the monomer interaction with: (a) pattern top, Λ_S^K; (b) with sidewall, Λ_W^K were defined. For most of the results, a strongly favorable sidewall interaction for B monomers and an unfavorable interaction for A monomers was employed, corresponding to $\Lambda_W^B N = -\Lambda_W^A N = 1.0$, and the top of the pattern was considered to be weakly repulsive to B and neutral to A i.e. $\Lambda_S^B N = -0.2$ and $\Lambda_S^A N = 0.0$. Such interactions were chosen so that a parallel orientation of B monomers along the top becomes unfavorable. The top of the confined film was defined as a neutral surface for both BCP components, $\Lambda_T^B N = -\Lambda_T^A N = 0.0$.

A non-dimensional representation was used, in which the lengthscales were normalized by the unperturbed radius of gyration, R_g, of the BCP chain. The invariant degree of polymerization was fixed as $\sqrt{N} = \rho_0(R_g/6)^3/N = 110$ (ρ_0 is the polymer segment density), $N = 32$, $\chi N = 25$ and $\kappa N = 35$. The period of the BCP in bulk for these conditions corresponds to $L_o = 4.06Rg$.[13] The thickness of the BCP film was varied in the range $1L_o - 2L_o$. The height of the pattern was fixed at $H_s = 1R_g$, the width of the pattern, W_s, was set to $W_s = 1L_o, 2L_o$ and the ability to achieve density multiplication was studied in the range $M = 2-8X$. The R_g of the random copolymer brush chains were varied between $0.25-1.0R_g$ which corresponds to number of polymer segments in the range $8-32$. Periodic boundary conditions were applied in X and Y direction whereas the BCP thin film boundary in the Z direction was assumed to be impenetrable. The simulation box was discretized into a three-dimensional grid. In the SCMF framework, the grid spacing (or discretization) is a lengthscale below which the correlations among polymer segments are ignored. Utilizing a grid spacing much smaller than the bond length would mean that the polymer segments would barely interact. On the other hand, a grid spacing much larger than the bond length would result in an inadequate resolution in inhomogeneous monomer densities. Hence, the grid spacing was set at $0.36R_g$ that was comparable to bond length as an optimum balance. The range of interaction for the short range potential acting on a monomer in the vicinity of a hard wall was also fixed at $0.36R_g$. The use of grid spacing as the interaction range of short range potential is justified by noting that the smallest lengthscale of interactions is the grid spacing below which correlations are ignored.

The model described above was used in a MC simulation approach wherein the configurational space was sampled using the Metropolis algorithm.[55] The initial configuration consisted of random orientation of the BCP and grafted random copolymer chains. The monomer positions were evolved in three dimensions using random displacement MC moves. In addition to monomer displacement moves, global moves such as slithering snake and

chain translation moves were used to enable faster equilibration. After every MC step (i.e. one MC attempt per monomer), the fields $w(r_i(s)), \pi(r_i(s))$ were updated based on the inhomogeneous volume fractions of the A and B monomers. The system was equilibrated for 5×10^5 MCS per monomer and the monomer densities were averaged after every MCS in order to analyze the morphologies. To determine the stability of morphologies formed in the simulations, free energy calculations are necessary, which are beyond the scope of this work. Instead, the simulations were repeated at least five times with different random initial conditions and the morphology formed in the majority of the cases is reported. In order to test if such a criteria is sufficient to deduce the most probable morphology, some simulations were repeated for additional five simulations. The most preferred morphology was seen to be insensitive to such number of repeat simulations. Similar considerations have been used in other work to identify the self-assembly characteristics.[48]

3 Results and discussion

In this section, the results for DSA of BCPs on topographically patterned substrates having sidewall interactions are presented. The objective was to identify conditions leading to the perpendicular lamellar morphology required for DSA. As stated in the introduction, the DSA strategy examined here utilizes a patterned substrate (having a pattern of lines of finite thickness) arranged parallel to one of the sides of the BCP thin film (see Figure 2). In such a system, there are a number of parameters which can be independently tuned to improve self assembly. Such variables include: (i) Polymer brush properties such as radius of gyration of the brush chains (B_{R_g}) and grafting density (σ); (ii) Pattern properties such as pattern height (H_s), width (W_s), strength of interaction (Λ_W^B); and (iii) BCP film thickness (L_z). These variables were systematically studied and their effect on the resulting BCP morphology and the density multiplication that can be achieved was examined.

3.1 Effect of brush size

Since DSA using patterned sidewalls is achieved by preferential wetting of the sidewall, a significant portion of the sidewall needs to be exposed after the brush backfilling.[27] Thus, the backfilling brush size was purposely kept short in order to produce a shallow trench between the top of the brush and top of the pattern surface. In this section, the influence of the size of the brush chains (in the range $B_{R_g} = 0.25 - 1$) on the alignment of BCP domains for fixed pattern height, $H_s = 1R_g$ was studied. The depth of the trench formed between backfilling brush and pattern surface (see Figure 2) was varied and the effect of the trench depth on the alignment of BCP domains was documented.

Figure 3 shows representative density profiles for DSA with 4X (a-b) and 6X (c-d) density multiplication for $W_s = 1L_o$ and $W_s = 2L_o$ respectively. The brown hashed region represents the pattern, whereas, the grey region denotes grafted random copolymer brushes. For clarity, only the volume fraction of the B component is displayed. In this model, the B component is preferential to the sidewall and hence aligns with the sidewall.

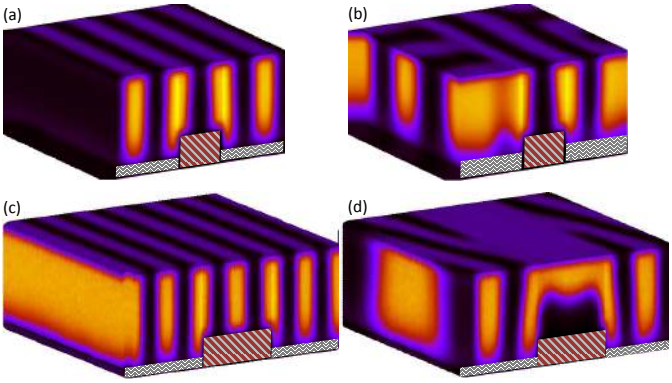

Fig. 3 Typical morphologies and density profiles obtained from SCMF simulations (only B monomer volume fraction is shown for clarity) for (a-b) 4X and (c-d) 6X density multiplication schemes for different pattern widths (a-b) $1L_o$ and (c-d) $2L_o$. The brown hashed region represents the substrate and grey patch denotes random copolymer brushes.

Figure 3(a) and 3(c) shows well-defined perpendicular morphology where the pattern is able to successfully guide the self-assembly, whereas, Figures 3(b) and 3(d) indicate mixed perpendicular morphologies wherein the pattern is able to guide the self-assembly only to a certain range, beyond which defects are seen in the lamellar morphology. For lithographic applications, the results of (a),(c) are desired whereas the results of (b),(d) are not suitable.

Figure 4 provides a summary of all of the results for the effect of the size of brush chains and grafting density on the morphology for density multiplication schemes in the range 2X-6X. For all of the examined grafting densities, 2X and 4X density multiplication were seen to be achievable irrespective of the actual brush size. For a 6X density multiplication scheme, an intermediate grafting density of $\sigma R_g^2 = 4$ is seen to be more successful in aligning defect free morphologies.

As stated in the introduction, the grafted copolymers differ from the hard walls as they represent a soft surface which can potentially modulate its thickness and the polymer segments can be rearranged to accommodate the self assembly. A previous study[51,52] demonstrated that the grafted copolymers can potentially create chemical inhomogeneities in both lateral and normal direction with respect to the substrate, thereby altering the surface energy to template/accommodate the self assembly. Such an effect was quantified using a local parameter termed compositional enrichment defined as $\phi_A(r)/f - \phi_B(r)/(1-f)$ where $\phi_{A/B}(r)$ denotes the volume fraction of A/B segments of the brush. A positive (negative) value of compositional enrichment denotes that the brush is locally enriched in A (B) component. Our results demonstrated that polymer brushes exhibiting high degrees of compositional enrichment also behave like a more "neutral" surface which facilitates perpendicular alignment.

Figure 5 shows the compositional enrichment for polymer brushes along the $X-$direction (averaged over Y and Z direction) for varying brush sizes at a fixed grafting density, $\sigma R_g^2 = 4$. The lines represent a moving average and are a guide to the eye. The compositional enrichment monotonically increases with increas-

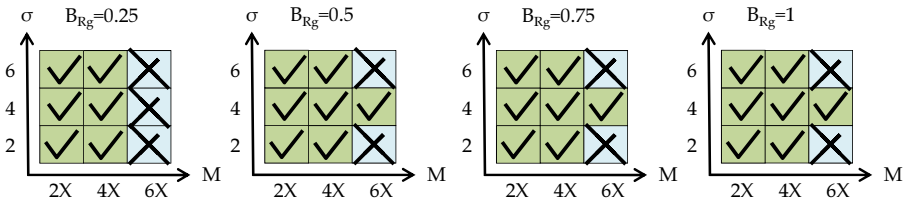

Fig. 4 Effect of the size of random copolymer brush chains and grafting density on density multiplication for $W_s = 1L_o$. The grafting density is denoted by σ defined as number of chains per unit area (R_g^2). The check marks denote aligned perpendicular lamellar morphology whereas cross represents a mixed perpendicular morphology.

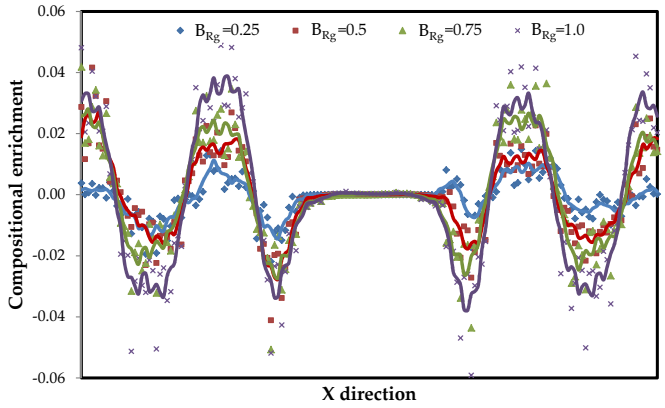

Fig. 5 Compositional enrichment averaged along Y and Z direction for varying size of brush chains for $\sigma R_g^2 = 4$.

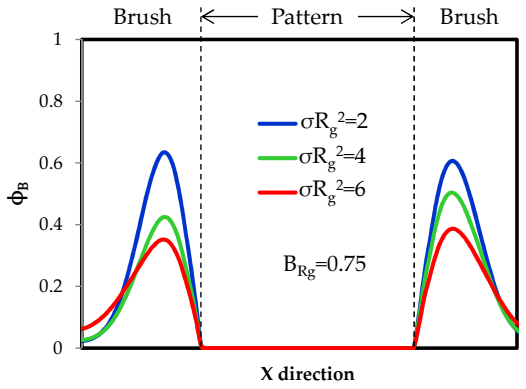

Fig. 6 BCP B monomer volume fractions (preferential to the sidewall) near the sidewall averaged along Y and Z direction for varying grafting densities. The average in the Z direction was performed between the substrate and top of the pattern.

ing brush size suggesting that longer brushes exhibit higher capacity of segmental rearrangements. Figure 4 shows that, short brushes ($B_{R_g} = 0.25$) are not able to form perpendicular BCP domains at $M = 6$X irrespective of the grafting density. Since the graft copolymer exhibits low compositional enrichment, it maybe that the compositional rearrangements of the random copolymer brush do not provide a sufficiently favorable surface for perpendicular alignment of the BCP.

Random copolymer brushes having $B_{R_g} = 0.5 - 1.0$ achieve 6X density multiplication but only at an intermediate grafting density of $\sigma R_g^2 = 4$. This result is likely a consequence of two competing features: (i) Longer grafted chains promote more conformational rearrangement (or high compositional enrichment) of brush segments leading to a more "neutral" surface. Hence, grafting densities as low as $\sigma R_g^2 = 2$ fail to provide a favourable surface in order to align the lamellar morphology along the guiding line. (ii) With increasing grafting density the exposure of the block copolymer segments near the pattern sidewall is reduced. To demonstrate this, Figure 6 displays the B segment volume fraction of the BCP near the sidewall (averaged along the Y direction) for varying grafting densities. The region showing zero volume fraction of B segments denotes the pattern with a sidewall interaction preferential to B segments. From Figure 6 it can be seen that, the volume fraction of B monomer deceases with increasing grafting density signifying reduced exposure of B monomers near the sidewall. This results in a reduction in the guiding strength offered by presence of the sidewall. Therefore, the 6X density multiplication can not be achieved at high grafting densities. Instead, the intermediate grafting density of $\sigma R_g^2 = 4$ seems to provide the balance of opposing factors mentioned above by providing sufficient exposure to the sidewall along with a sufficient compositional enrichment to support alignment of the lamellar domains.

Overall, self-assembly is seen to depend not only on the gap between brush surface and pattern surface (i.e. H_s, B_{R_g}) but also on the grafting density. The size of polymer brush needs to be sufficient to allow for a significant exposure of the sidewall for the BCP self assembly. The later is seen to be a function of both brush size and grafting density. An intermediate grafting density was seen to be most efficient in aligning lamellae for 6X density multiplication. Experimental work in this context has noted the importance of exposure of the sidewalls to the BCP segments.[27] These results indicate that, grafting density of the random copolymer brushes can also have a significant impact on the aligning efficiency of the patterns.

3.2 Effect of film thickness and pattern width

Figure 7 summarizes the results for two pattern widths, $W_s = 1L_o$ and $W_s = 2L_o$, and for varying BCP film thickness in the range $L_z = 1 - 2L_o$. In order to reduce the number of parameters, the simulations employed brush chains of size $B_{R_g} = 0.5$ and a grafting density of $\sigma R_g^2 = 6$ for all the results in this section. For

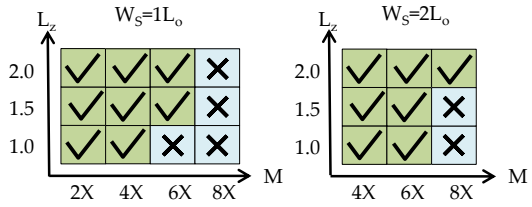

Fig. 7 Effect of BCP film thickness on density multiplication for pattern width of $1L_o$ and $2L_o$. The check marks denote perpendicular lamellar morphology whereas cross represent a mixed perpendicular morphology or morphology with defects.

$W_s = 1L_o$, the sidewall patterning is able to produce perpendicular morphology up to a density multiplication of 4X for all BCP film thicknesses between $L_z = 1 - 2L_o$, and up to 6X for BCP film thicknesses $L_z = 1.5, 2L_o$. Interestingly, wider patterns ($W_s = 2L_o$) are able to achieve 8X density multiplication for higher BCP film thickness. Since the sidewall guiding scheme utilizes two sidewalls per pattern as opposed to only one guiding surface (pattern top) employed in chemoepitaxy, the effectiveness of the pattern is seen to be substantially improved relative to the results reported for chemoepitaxy. With wider patterns, the spacing between sidewalls increases which delivers improved guiding efficiency. Hence, defect free aligned lamellar morphology is observed up to 8X density multiplication for wider patterns with $W_s = 2L_o$ which substantially reduces the demand for lithographic resolution.

For thinner films, most of the simulations show a mixed/defect morphology whereas better alignment is achieved for thicker films. It can be speculated that increasing film thickness would reduce the effects of confinement enabling the system to explore a larger conformational space. Since, excess free energy of defects in systems with vertically oriented lamellae is expected to increase with film thickness,[56] thinner films are likely to form defects. For instance, in the context of fingerprint patterns, Campbell *et al.* have observed that the defect density in quasi-2D lamellar patterns decreases with the film thickness.[57] Specifically, thinner films ($L_z < L_o$) were unable to annihilate the high energy defects that were less common in thicker films ($L_z > L_o$).[57] Such observations are consistent with results of Figure 7 demonstrating better alignment obtained with thicker BCP film.

In sum, the perpendicular alignment of lamellae with the guiding pattern becomes more favorable with increasing BCP film thickness. For the set of parameters examined in this study, wider guiding stripes ($W_s = 2L_o$) are seen to achieve density multiplication up to 8X for thicker BCP films ($L_z = 2L_o$). This is a consequence of better guiding strength (two guiding lines per pattern) offered by wider patterns. However, such improvement in alignment with wider patterns is likely to have an upper bound until which an improvement in guiding strength is observed.

3.3 Effect of sidewall interaction strength

Next, the DSA of BCP for $\Lambda_W^B N = 0.5, 1.0, 2.0$ is examined as a function of BCP film thickness to test whether the self assembly improves/deteriorates as a function of strength of sidewall interaction. Figure 8 shows the results for varying film thickness and sidewall interactions for $W_s = 1L_o - 2L_o$. Overall, increasing the sidewall interaction is seen to monotonically improve vertical alignment of lamellae. The attraction (repulsion) between sidewall and B (A) segments increases with Λ_W^B. Thus higher Λ_W^B results in a higher effective repulsion between A and B segments at the interface near the sidewall leading to better guiding of BCP domains. In some cases, the increased strength of interaction is seen to enable alignment for a higher density multiplication scheme. For instance, 6X density multiplication can be achieved only with higher strength of sidewall interaction $\Lambda_W^b N = 1.0, 2.0$ for $L_z = 1.5L_o$ ($W_s = 1L_o$) and $L_z = 1L_o$ ($W_s = 2L_o$). Similarly, 8X density multiplication can be achieved only with the highest strength of sidewall interaction studied in this section, $\Lambda_W^b N = 2.0$ for $L_z = 1.5L_o$ ($W_s = 2L_o$). Consistent with the effect of film thickness seen in the previous section, better self assembly was observed for higher BCP film thicknesses. For $W_s = 1L_o$ and $W_s = 2L_o$, density multiplication up to 6X and 8X rendered the desired morphologies for film thickness of $L_z = 2L_o$ as opposed to the 4X ($W_s = 1L_o$) and 6X ($W_s = 2L_o$) density multiplication achieved with $L_z = 1L_o$. Interestingly, even 8X density multiplication can be achieved for all values of sidewall interaction strengths with wider chemical patterns at $L_z = 2L_o$.

An interesting question is whether the key parameter driving the alignment is the interaction energy of the side wall by itself or whether the controlling factor is the product of the interaction energy and the exposed area of the side wall. In order to examine the specific role of exposed area of sidewall, a case in which the pattern height H_s was doubled was considered ($H_s = 2R_g$). Correspondingly, the side wall interaction parameter was reduced by half to maintain the product of area of sidewall and interaction parameter a constant. The height of the brush was also scaled with respect to pattern height. The results for such parameters are displayed in Figure 9. In comparing with the results displayed in Figure 8, we observe that the vertical alignment of lamellae deteriorates for a higher pattern height (i. e. lower sidewall interaction but the same product of area of sidewall and sidewall interaction parameter). Moreover, the lowest interaction strength of $\Lambda_W^b N = 0.25$ is unable to guide the self assembly even for a density multiplication of 2X. These results, albeit not comprehensive, serve to demonstrate that the side wall interaction energy by itself serves as an important parameter in determining the alignment influence of the patterns.

Overall, chemical patterns with appropriate sidewall interactions are able to guide the self assembly over longer periods as compared to chemoepitaxy while extending the pattern width regimes to $W_s = 2L_o$. Moreover, in some cases, increased strength of sidewall interactions enables alignment for higher density multiplication schemes than that have been achieved in experiments. Such results motivate experiments which can more thoroughly explore the parameters underlying the sidewall patterning scheme to probe if indeed such multiplication schemes can be realized in practice.

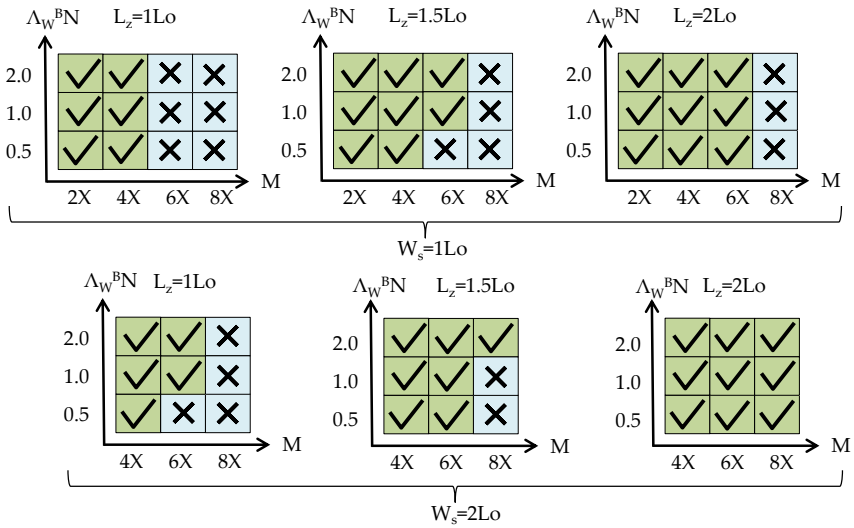

Fig. 8 Effect of sidewall interaction on density multiplication for pattern height of $H_s = 1R_g$ and pattern width of $W_s = 1L_o$ and $W_s = 2L_o$ for varying sidewall interaction strength. The check marks denote perpendicular lamellar morphology whereas cross represent a mixed perpendicular morphology.

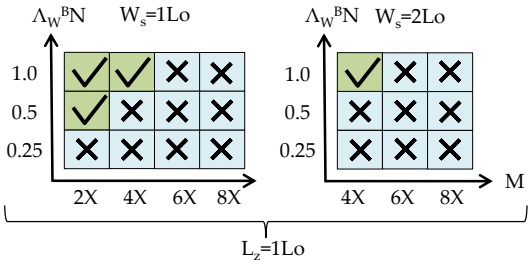

Fig. 9 Effect of sidewall interaction on density multiplication for pattern width of $W_s = 1L_o$ and $W_s = 2L_o$ and pattern height of $H_s = 2R_g$ for varying sidewall interaction strength. The check marks denote perpendicular lamellar morphology whereas cross represent a mixed perpendicular morphology.

4 Summary

The DSA of lamellae forming BCPs on patterned substrates having sidewall interactions was studied using a coarse grained polymer model wherein the backfill polymer brushes were modeled explicitly. The effect of brush properties, BCP film thickness and pattern width on the BCP morphologies were examined. An intermediate size of random copolymer brush (relative to the height of the pattern), which allows local composition modulation of the brush simultaneously with significant exposure of sidewall was predicted to be optimum for DSA. The effect of BCP film thickness for density multiplication schemes $2-8$X was examined for pattern widths of $1-2L_o$. Patterns having $W_s = 1L_o$ guide self-assembly up to 4X density multiplication (i.e. pattern period of $4L_o$) whereas patterns with $W_s = 2L_o$ orient lamellae up to 8X density multiplication. Thicker BCP films are seen to orient lamellae for large periods of patterns. It appears that thicker BCP films are less likely to get trapped in metastable configurations and hence, achieve alignment up to 8X density multiplications for wider patterns. Overall theses results indicate that the sidewall patterning scheme greatly reduces the lithography resolution requirements and has significant potential to direct the self assembly of block copolymer with wider pattens having density multiplication of 8X. Moreover, unlike chemoepitaxy, where density multiplication only up to 4X can be achieved with a proper tuning to brush chemistry, the patterned sidewall scheme achieves density multiplication schemes (up to 8X) over a range of BCP film thicknesses, sidewall interactions without tuning polymer brush properties such as composition, size and grafting density.

5 Acknowledgement

This work was supported in part by grants from Robert A. Welch Foundation (grant #$F1599$ to VG, grant #$F1709$ to CJE), National Science Foundation (DMR-1306844 to VG), the US Army Research Office under grant W911NF-13-1-0396 (to VG), Nissan Chemical Company (to CGW), and the Rashid Engineering Regents Chair (to CGW). We thank Dr. Victor Pryamitsyn for useful discussions. The authors acknowledge the Texas Advanced Computing Center (TACC) at The University of Texas at Austin for providing computing resources that have contributed to the research results reported within this paper.

References

1 D. J. C. Herr, *Journal of Materials Research*, 2011, **26**, 122–139.
2 M. P. Stoykovich and P. F. Nealey, *Materials Today*, 2006, **9**, 20–29.
3 S. B. Darling, *Progress In Polymer Science*, 2007, **32**, 1152–1204.
4 C. M. Bates, M. J. Maher, D. W. Janes, C. J. Ellison and C. G. Willson, *Macromolecules*, 2014, **47**, 2–12.
5 R. Ruiz, E. Dobisz and T. R. Albrecht, *Acs Nano*, 2011, **5**, 79–84.

6 H. Yi, X.-Y. Bao, J. Zhang, C. Bencher, L.-W. Chang, X. Chen, R. Tiberio, J. Conway, H. Dai, Y. Chen, S. Mitra and H. . S. P. Wong, *Advanced Materials*, 2012, **24**, 3107–3114.

7 H. Tsai, J. W. Pitera, H. Miyazoe, S. Bangsaruntip, S. U. Engelmann, C.-C. Liu, J. Y. Cheng, J. J. Bucchignano, D. P. Klaus, E. A. Joseph, D. P. Sanders, M. E. Colburn and M. A. Guillorn, *Acs Nano*, 2014, **8**, 5227–5232.

8 X. M. Yang, R. D. Peters, P. F. Nealey, H. H. Solak and F. Cerrina, *Macromolecules*, 2000, **33**, 9575–9582.

9 S. O. Kim, H. H. Solak, M. P. Stoykovich, N. J. Ferrier, J. J. de Pablo and P. F. Nealey, *Nature*, 2003, **424**, 411–414.

10 R. Ruiz, H. Kang, F. A. Detcheverry, E. Dobisz, D. S. Kercher, T. R. Albrecht, J. J. de Pablo and P. F. Nealey, *Science*, 2008, **321**, 936–939.

11 M. P. Stoykovich, M. Muller, S. O. Kim, H. H. Solak, E. W. Edwards, J. J. de Pablo and P. F. Nealey, *Science*, 2005, **308**, 1442–1446.

12 F. A. Detcheverry, G. Liu, P. F. Nealey and J. J. de Pablo, *Macromolecules*, 2010, **43**, 3446–3454.

13 C.-C. Liu, A. Ramirez-Hernandez, E. Han, G. S. W. Craig, Y. Tada, H. Yoshida, H. Kang, S. Ji, P. Gopalan, J. J. de Pablo and P. F. Nealey, *Macromolecules*, 2013, **46**, 1415–1424.

14 G. Garner, L. Williamson, R. Seidel, P. R. Delgadillo, S.-M. Hur, R. L. Gronheid, P. F. Nealey and J. J. de Pablo, *Alternative Lithographic Technologies Vii*, 2015, **9423**, SPIE; DNS Elect LLC.

15 P. Mansky, Y. Liu, E. Huang, T. P. Russell and C. J. Hawker, *Science*, 1997, **275**, 1458–1460.

16 E. Huang, T. P. Russell, C. Harrison, P. M. Chaikin, R. A. Register, C. J. Hawker and J. Mays, *Macromolecules*, 1998, **31**, 7641–7650.

17 F. A. Detcheverry, P. F. Nealey and J. J. de Pablo, *Macromolecules*, 2010, **43**, 6495–6504.

18 B. D. Terris, *Journal of Magnetism and Magnetic Materials*, 2009, **321**, 512–517.

19 T. R. Albrecht, D. Bedau, E. Dobisz, H. Gao, M. Grobis, O. Hellwig, D. Kercher, J. Lille, E. Marinero, K. Patel, R. Ruiz, M. E. Schabes, L. Wan, D. Weller and T.-W. Wu, *IEEE Transactions on Magnetics*, 2013, **49**, 773–778.

20 Y. S. Jung and C. A. Ross, *Nano Letters*, 2007, **7**, 2046–2050.

21 S. Park, D. H. Lee, J. Xu, B. Kim, S. W. Hong, U. Jeong, T. Xu and T. P. Russell, *Science*, 2009, **323**, 1030–1033.

22 J. D. Cushen, I. Otsuka, C. M. Bates, S. Halila, S. Fort, C. Rochas, J. A. Easley, E. L. Rausch, A. Thio, R. Borsali, C. G. Willson and C. J. Ellison, *Acs Nano*, 2012, **6**, 3424–3433.

23 J. D. Cushen, C. M. Bates, E. L. Rausch, L. M. Dean, S. X. Zhou, C. G. Willson and C. J. Ellison, *Macromolecules*, 2012, **45**, 8722–8728.

24 M. J. Maher, C. T. Rettner, C. M. Bates, G. Blachut, M. C. Carlson, W. J. Durand, C. J. Ellison, D. P. Sanders, J. Y. Cheng and C. G. Willson, *ACS Applied Materials & Interfaces*, 2015, **7**, 3323–3328.

25 W. J. Durand, G. Blachut, M. J. Maher, S. Sirard, S. Tein, M. C. Carlson, Y. Asano, S. X. Zhou, A. P. Lane, C. M. Bates, C. J. Ellison and C. G. Willson, *Journal of Polymer Science Part A-polymer Chemistry*, 2015, **53**, 344–352.

26 J. Kim, J. Wan, S. Miyazaki, J. Yin, Y. Cao, Y. J. Her, H. Wu, J. Shan, K. Kurosawa and G. Lin, *Journal of Photopolymer Science and Technology*, 2013, **26**, 573–579.

27 J. Cushen, L. Wan, G. Blachut, M. J. Maher, T. R. Albrecht, C. J. Ellison, C. G. Willson and R. Ruiz, *ACS Applied Materials & Interfaces*, 2015, 13476–13483.

28 M. Muller and G. D. Smith, *Journal Of Polymer Science Part B-Polymer Physics*, 2005, **43**, 934–958.

29 K. C. Daoulas and M. Muller, *Journal Of Chemical Physics*, 2006, **125**, 184904.

30 K. C. Daoulas, M. Muller, J. J. de Pablo, P. F. Nealey and G. D. Smith, *Soft Matter*, 2006, **2**, 573–583.

31 K. C. Daoulas, M. Muller, M. P. Stoykovich, H. Kang, J. J. de Pablo and P. F. Nealey, *Langmuir*, 2008, **24**, 1284–1295.

32 J. Wang and M. Muller, *Macromolecules*, 2009, **42**, 2251–2264.

33 J. F. Wang and M. Muller, *Journal Of Physical Chemistry B*, 2009, **113**, 11384–11402.

34 J. F. Wang and M. Muller, *Langmuir*, 2010, **26**, 1291–1303.

35 B. Steinmuller, M. Muller, K. R. Hambrecht, G. D. Smith and D. Bedrov, *Macromolecules*, 2012, **45**, 1107–1117.

36 B. Narayanan, V. A. Pryamitsyn and V. Ganesan, *Macromolecules*, 2004, **37**, 10180–10194.

37 B. Narayanan and V. Ganesan, *Physics Of Fluids*, 2006, **18**, 042109.

38 F. A. Detcheverry, H. M. Kang, K. C. Daoulas, M. Muller, P. F. Nealey and J. J. de Pablo, *Macromolecules*, 2008, **41**, 4989–5001.

39 F. A. Detcheverry, D. Q. Pike, U. Nagpal, P. F. Nealey and J. J. de Pablo, *Soft Matter*, 2009, **5**, 4858–4865.

40 S. W. Sides, B. J. Kim, E. J. Kramer and G. H. Fredrickson, *Physical Review Letters*, 2006, **96**, 250601.

41 N. A. Kumar and V. Ganesan, *Journal Of Chemical Physics*, 2012, **136**, 101101.

42 M. P. Stoykovich, H. Kang, K. C. Daoulas, G. Liu, C.-C. Liu, J. J. de Pablo, M. MÃČÂijller and P. F. Nealey, *ACS Nano*, 2007, **1**, 168–175.

43 M. Muller and K. Daoulas, *Macromolecular Symposia*, 2007, **252**, 68–75.

44 M. Muller, W. Li and O. J. Rey, *MRS Proceedings*, 2015, **175**, –.

45 Q. Wang, Q. Yan, P. F. Nealey and J. J. de Pablo, *Macromolecules*, 2000, **33**, 4512–4525.

46 E. W. Edwards, M. Muller, M. P. Stoykovich, H. H. Solak, J. J. de Pablo and P. F. Nealey, *Macromolecules*, 2007, **40**, 90–96.

47 G. Liu, F. Detcheverry, A. Ramírez-Hernández, H. Yoshida, Y. Tada, J. J. de Pablo and P. F. Nealey, *Macromolecules*, 2012, **45**, 3986–3992.

48 A. Ramírez-Hernández, G. Liu, P. F. Nealey and J. J. de Pablo, *Macromolecules*, 2012, **45**, 2588–2596.

49 V. V. Ginzburg, J. D. Weinhold, P. D. Hustad and I. Trefonas, Peter, *Journal of Photopolymer Science and Technology*, 2013, **26**, 817–823.

50 A. Ramírez-Hernández, H. S. Suh, P. F. Nealey and J. J. de Pablo, *Macromolecules*, 2014, **47**, 3520–3627.
51 D. M. Trombly, V. Pryamitsyn and V. Ganesan, *Macromolecules*, 2011, **44**, 9867–9881.
52 D. M. Trombly, V. Pryamitsyn and V. Ganesan, *Physical Review Letters*, 2011, **107**, 148304–1–5.
53 G. H. Fredrickson, *The equilibrium theory of inhomogeneous polymers*, Oxford University Press, 2006.
54 G. H. Fredrickson, S. T. Milner and L. Leibler, *Macromolecules*, 1992, **25**, 6341–6354.
55 N. Metropolis, A. Rosenbluth, M. Rosenbluth, A. Teller and E. Teller, *Journal of Chemical Physics*, 1953, **21**, 1087–1092.
56 W. Li and M. Muller, *Annual Review of Chemical and Biomolecular Engineering*, 2015, **6**, 9.1–9.30.
57 I. P. Campbell, S. Hirokawa and M. P. Stoykovich, *Macromolecules*, 2013, **46**, 9599–9608.

Short Abstract: Directed self-assembly of block copolymers on chemical patterns with sidewall guiding lines is examined using single chain in mean field simulations. The sidewall guiding strategy substantially reduces the resolution requirement by utilizing wider patterns up to two periods of the lamellar domains. Vertical alignment was achieved for film thickness between one to two periods of block copolymer and our results demonstrate density multiplication up to 8X.

1 line TOC Entry: Directed self-assembly of block copolymers on chemical patterns with sidewall guiding lines is examined as a function of backfill brush properties, block copolymer film thickness, pattern size, and sidewall interaction strength.